

## AEGIS: A PANCHROMATIC STUDY OF IRAC-SELECTED EXTREMELY RED OBJECTS WITH CONFIRMED SPECTROSCOPIC REDSHIFTS

G. WILSON<sup>1</sup>, J.-S. HUANG<sup>2</sup>, G. G. FAZIO<sup>2</sup>, R. YAN<sup>3</sup>, A. M. KOEKEMOER<sup>4</sup>, S. SALIM<sup>5</sup>, S. M. FABER<sup>6</sup>, J. LOTZ<sup>6</sup>, C. N. A. WILLMER<sup>7</sup>, M. DAVIS<sup>3</sup>, A. L. COIL<sup>7,8</sup>, J. A. NEWMAN<sup>8,9</sup>, C. J. CONSELICE<sup>10</sup>, C. PAPOVICH<sup>7</sup>, M. L. N. ASHBY<sup>2</sup>, P. BARMBY<sup>2</sup>, S. P. WILLNER<sup>2</sup>, R. IVISON<sup>11</sup>, S. MIYAZAKI<sup>12</sup>, AND D. RIGOPOULOU<sup>13</sup>

*Draft version September 21, 2018*

### ABSTRACT

We study 87 Extremely Red Objects (EROs), selected both to have color redder than  $R - [3.6] = 4.0$ , and to have confirmed spectroscopic redshifts. Together, these two constraints result in this sample populating a fairly narrow redshift range at  $0.76 < z < 1.42$ . The key new ingredient included here is deep *Spitzer* Space Telescope InfraRed Array Camera (IRAC) data. Based on  $[3.6] - [8.0]$  color, we demonstrate that it is possible to classify EROs into early-type, dusty starburst, or power-law (AGN) types. We present ultraviolet to mid-infrared spectral energy distributions (SEDs) and Advanced Camera for Surveys (ACS) images, both of which support our simple IRAC color classification.

*Subject headings:* galaxies: evolution — galaxies: high-redshift — infrared: galaxies — galaxies: elliptical and lenticular, cD — galaxies: starburst

### 1. INTRODUCTION

First discovered in the late 1980s (Elston et al. 1988), extremely red objects (EROs) are defined by their very red optical/near-infrared colors. It has been known for some time that the redness of their color constrains these galaxies to be either early-type galaxies, starburst galaxies reddened by dust, or AGN (or a combination of these three classes). However, until recently, with observations limited to  $K$ -band (or shorter wavelengths), it has proven extremely challenging to accurately classify the EROs by type (Mannucci et al. 2002), even in combination with high-resolution HST imaging (Moustakas et al. 2004).

Although EROs appear to consist of a heterogeneous mix of galaxy classes, the emerging paradigm is that they may well be the high redshift counterparts and progenitors of local massive E and SO galaxies. Their reliable classification and study, especially at intermediate redshift ( $z \sim 1$ ) can provide crucial constraints on the evolution of massive, starburst, dusty and/or ultra-luminous infrared galaxies (ULIRGs) known to exist at

higher redshift e.g., BzKs (Daddi et al. 2004), BX/BMs (Reddy et al. 2005), Distant Red Galaxies (Franx et al. 2003; Papovich et al. 2006; Conselice 2006, DRGs), sub-millimeter and IR-Luminous Lyman Break Galaxies (Huang et al. 2005; Rigopoulou 2006, ILLBGs).

In the restframe near-IR, old stellar populations show a turndown at wavelengths longer than the restframe  $1.6\mu\text{m}$  ‘bump’, while dusty starburst populations show emission from small hot dust grains. AGN-dominated sources display a power-law spectral energy distribution. In Wilson et al. (2004) we showed how data from *Spitzer* could begin to help distinguish among different ERO populations. In this paper, we extend our ERO study to take advantage of the rich panchromatic dataset available from the All-wavelength Extended Groth strip International Survey (AEGIS). All magnitudes used in this letter are AB, unless otherwise specified.

### 2. THE AEGIS DATASET

The *Spitzer* IRAC (3.6, 4.5, 5.7,  $8.0\mu\text{m}$ , Fazio et al. 2004) component of the Extended Groth Strip (EGS) survey spans an area of  $120 \times 10$  arcmin (Huang et al. 2006, in prep: see also Huang et al. 2004; Barmby et al. 2006; Huang 2006). In conducting this ERO study, we also utilized DEEP2 spectroscopy (Davis et al. 2006, in prep), and  $u'g'$  (Ashby et al. 2006, in prep), CFHT *BRI* (Coil et al. 2004), ACS  $V(F606W)$  and  $I(F814W)$ , deep Subaru  $R$  (Miyazaki et al. 2002, 27.0 AB,  $5\sigma$ ),  $K$  (Conselice et al. 2006, in prep), and *Spitzer* Multiband Imaging Photometer (MIPS, Rieke et al. 2004)  $24\mu\text{m}$  imaging. Further details may be found in Davis et al. (2006).

### 3. IRAC-SELECTED GALAXIES AND THEIR COLOR-COLOR DISTRIBUTION

The EGS field contains  $\sim 45000$  galaxies detected at  $3.6\mu\text{m}$  (23.9 AB,  $5\sigma$ ). Figure 1 shows an  $R - [3.6]$  versus  $[3.6] - [8.0]$  color-color diagram. The black points show the  $\sim 13000$   $3.6\mu\text{m}$ -selected galaxies with both good quality Subaru  $R$  and  $8.0\mu\text{m}$  photometry.

The colored tracks on Figure 1 show the location in color-color space as a function of redshift ( $0 < z < 4$ )

arXiv:astro-ph/0608447v1 21 Aug 2006

<sup>1</sup> Spitzer Science Center, California Institute of Technology, 220-6, Pasadena, CA 91125; gillian@ipac.caltech.edu

<sup>2</sup> Harvard-Smithsonian Center for Astrophysics, 60 Garden Street, Cambridge, MA 02138

<sup>3</sup> Department of Astronomy, University of California Berkeley, Campbell Hall, Berkeley, CA94720

<sup>4</sup> Space Telescope Science Institute, 3700 San Martin Drive, Baltimore, MD 21218

<sup>5</sup> Department of Physics and Astronomy, University of California Los Angeles, Knudsen Hall, Los Angeles, CA 90095

<sup>6</sup> UCO/Lick Observatory and Department of Astronomy and Astrophysics, University of California Santa Cruz, 1156 High Street, Santa Cruz, CA 95064

<sup>7</sup> Steward Observatory, University of Arizona, Tucson, AZ 85721

<sup>8</sup> Hubble Fellow

<sup>9</sup> Institute for Nuclear and Particle Astrophysics, Lawrence Berkeley National Laboratory, Berkeley, CA 94700

<sup>10</sup> The School of Physics and Astronomy, University of Nottingham, University Park, Nottingham NG7 2RD, UK

<sup>11</sup> Astronomy Technology Centre, Royal Observatory, Blackford Hill, Edinburgh EH9 3HJ, U.K.

<sup>12</sup> Subaru Telescope, National Astronomical Observatory of Japan, 650 North A'ohoku Place, Hilo, HI 96720

<sup>13</sup> Department of Astrophysics, Oxford University, Keble Road, Oxford, OX1 3RH, United Kingdom

for eight non-evolving empirical templates (four common Coleman, Wu, & Weedman 1980 (CWW) templates [E, Sbc, Scd, Im] empirically extended to  $10\mu\text{m}$  using ISO data (Huang et al., 2006, in prep), a dusty starburst template [M82], a dusty starburst/ULIRG template [Arp220], and two AGN templates [NGC 1068 and NGC 5506]). While we fully expect these templates to become increasingly inaccurate at high redshift, they do serve to provide simple insight onto the likely nature and redshift distribution of galaxies within this color-color diagram.

A distinctive swath of galaxies is clearly apparent curving from the left to the top of Figure 1 (the plume in the lower left corner is caused by stellar contamination). Notice, especially, the excellent agreement between this swath of galaxies observed in color-color space and the CWW E (blue) track to  $z \sim 0.7$ , when the template noticeably begins to diverge from the “bluer” data. We note that the predictability of the  $[R] - [3.6]$  color-redshift relation for early-type galaxies can be utilized as an effective technique for detecting high redshift clusters of galaxies e.g., at  $z < 1.4$  in the  $4\text{ deg}^2$  Spitzer First Look Survey Field (Wilson et al. 2005; Muzzin et al, 2006, in prep). The SpARCS collaboration<sup>14</sup> is currently utilizing an even redder  $[z'] - [3.6]$  color to detect and study clusters to  $z = 2$  in the  $50\text{ deg}^2$  Spitzer SWIRE Legacy Fields (Wilson et al. 2006).

We *define* an ERO to be a galaxy redder in color than  $R - [3.6] = 4.0$ . This is the same criterion used in Wilson et al. (2004), and is a very similar selection criterion to the traditional Vega  $R - K > 5.0$  requirement (see Wilson et al. 2004 for a discussion).

From Figure 1, we might expect that only high redshift ( $z \gtrsim 0.8$ ) early-type, ( $z \gtrsim 1.0$ ) dusty starburst galaxies, and AGN (at any redshift) would satisfy this extremely red criterion. As we shall demonstrate in the remainder of this letter, this indeed turns out to be the case. Note that late-type CWW Scd (cyan) and irregular (purple) galaxies are *never* sufficiently red to be classified as an ERO *at any redshift*, and one would not expect to find any CWW late-type Sbc (green) EROs at  $z < 1.5$ .

#### 4. REDSHIFT DISTRIBUTION OF THE SPECTROSCOPIC ERO SAMPLE

There are several thousand EROs in the EGS field. Here, we carry out a pilot study of the 87 EROs with confirmed DEEP2 spectroscopic redshifts. We use spectroscopy in this letter only for redshift determination.

The solid black histogram in the far left panel of Figure 2 shows the redshift distribution of the 87 EROs in our sample. The EROs occupy a relatively narrow redshift range at  $0.76 < z < 1.42$ . The dotted black histogram shows the redshift distribution of those galaxies in the DEEP2 EGS field with good quality spectroscopic redshift determinations (scaled down by a factor of 15).

The fact that none of the EROs are located at  $z < 0.76$  is not a DEEP2 selection effect; in EGS, DEEP2 samples the full redshift range  $0 < z < 1.45$  (Faber 2006; Willmer 2006). It is caused by the additional ERO  $R - [3.6] > 4.0$  selection requirement, which effectively excludes low redshift galaxies (Figure 1). The DEEP2+ERO selection function also limits this sample to a fairly bright but nar-

row range of  $18.5 < [3.6] < 20$ , with the one exception of 12007954, a 17th magnitude AGN (Le Floch 2006). Note that by selecting only those EROs with spectroscopic redshifts, we may bias our sample against inclusion of any low-redshift extremely dusty galaxies (since optically faint galaxies will not pass the  $R < 24.1$  selection requirement of the DEEP2 survey).

#### 5. ERO CLASSIFICATION USING $[3.6] - [8.0]$ COLOR

It is possible to divide the EROs in this sample into three broad classes by means of their IRAC  $[3.6] - [8.0]$  color. In this section, we introduce each of these classes, show examples of their SEDs and discuss the sometime subtle features which are only apparent from such broad-baseline datasets. We also study their morphologies using ACS images.

From Figure 1, early-type galaxies are expected to have the bluest ( $[3.6] - [8.0] \simeq -1.0$ ) colors, dusty starburst galaxies intermediate colors ( $[3.6] - [8.0] \simeq -0.5$ ), and AGN reddest colors ( $[3.6] - [8.0] \simeq +1.0$ ). The right panel of Figure 2 corresponds to the dashed rectangle in Figure 1 and shows the subsample of 87 EROs with spectroscopic redshifts. We *classify*  $[3.6] - [8.0] < -0.75$  galaxies as bulge-dominated early types (blue circles),  $-0.75 < [3.6] - [8.0] > 0.0$  galaxies as dusty starburst<sup>15</sup> (red triangles) and  $[3.6] - [8.0] < 0.0$  galaxies as power-law AGN types (orange boxes). As we shall demonstrate, these two simple color cuts do separate the classes rather well. This is because the redshift distribution of this particular sample is rather narrow. For a sample spanning a broader redshift distribution, one might imagine utilizing a more complex color selection to isolate the meanderings of the different populations through color-color space in Figure 1.

We classify 53 of the EROs as early types. They are located at  $0.82 < z < 1.28$  and their redshift distribution is shown by the blue hatching in the middle panel of Figure 2. We classify 32 EROs as being dusty starburst types. The dusty starburst population (shown by the red hatching) has a slightly wider redshift distribution from  $0.76 < z < 1.42$  (presumably because galaxies in this class can contain arbitrary amounts of dust). We classify two EROs as being predominantly power-law types. These are 12007878 at  $z = 0.99$  and 12007954 at  $z = 1.15$ , and are shown in solid orange (see also Konidaris 2006).

#### 6. EXAMPLE SPECTRAL ENERGY DISTRIBUTIONS AND ACS IMAGES

Figures 3 and 4 (Plate 1) show examples of observed SEDs and  $3'' \times 3''$  *I*-band (F814W) postage stamp ACS images. For comparison, also shown are CWW E (blue) and M82 (red) templates (§ 3) as they would appear at the redshift of each ERO. At  $z \sim 1$ , IRAC’s  $8\mu\text{m}$  channel measures any emission from small hot dust grains (indicative of a dusty starburst galaxy) while the  $3.6\mu\text{m}$  channel measures the stellar peak. A relative red (or blue)  $[3.6] - [8.0]$  color, therefore, can be used to discriminate for (or against) dusty starburst galaxies (and AGN) at this redshift.

<sup>15</sup> We use the word “starburst” to mean a galaxy whose IR luminosity is powered by star formation. We do not intend to imply these galaxies have total IR luminosity  $L(8 - 1000\mu\text{m}) < 10^{11} L_{\odot}$ . Indeed, as we shall discuss in § 7 most of these dusty starburst EROs would actually be classified as LIRGs.

<sup>14</sup> <http://spider.ipac.caltech.edu/staff/gillian/SpARCS>

### 6.1. Early-Type EROs

Figure 3 (Plate 1) shows six examples of galaxies IRAC color-classified as early-type EROs. The CWW E template approximates the 13048898, 13019047, 13004276, and 12004426 SEDs very well. The CWW E template appears to underestimate the SEDs of 13019309 and 12008091 in the UV. In all cases the ACS images show clear evidence of bulge-dominated morphologies, supporting our color classification as early types.

A total of 35 of the 53 early-type EROs fall within the ACS footprint. A close inspection of all of the available ACS images reveals them to be predominantly bulge-dominated (E, S0 or Sa-type spirals). A small number ( $\sim 10\%$ ) appear to be undergoing mergers. We conclude that choosing a blue [3.6]-[8.0] color successfully selects for  $z = 1$  EROs with old stellar populations and against those with dusty starburst or power-law features.

### 6.2. Dusty Starburst and Power-Law EROs

Figure 4 (Plate 1) shows five examples of galaxies IRAC color-classified as dusty starburst EROs, and one power-law ERO (12007878). The M82 template approximates the SEDs of sources 13042940, 12100899, and 12007831 very well, and that of 13004291 reasonably well. In addition to being more mid-IR luminous than an early-type ERO of similar  $3.6\mu\text{m}$  magnitude, the SEDs of these four sources are more luminous in the optical. Their ACS images show clear evidence of disturbed, peculiar, interacting or merging galaxies.

Neither template approximates well the SED of 12008048. Close inspection of the ACS image reveals it to be a face-on spiral galaxy. Since a normal spiral at  $z = 0.9$  would not meet the  $R - [3.6]$  redness criterion, we infer that 12008048 must be an especially dusty spiral.

A total of 17 of the 32 EROs we classify as dusty starbursts fall within the ACS footprint. Close inspection of all of their images reveals many of them ( $\sim 60\%$ ) to be disturbed or interacting galaxies, and the remainder ( $\sim 40\%$ ) to be late-type spirals.

12007878 shows a monotonically increasing power-law SED. Its host galaxy is clearly bulge-dominated and it can be unequivocally classified as an AGN-dominated source.

## 7. DISCUSSION

Turning to those EROs which have  $24\mu\text{m}$  detections, there are five ( $17.4 < [24] < 19.1$ ) amongst the 53 early-type and 29 ( $16.8 < [24] < 19.1$ ) amongst the 32 dusty starburst EROs. Both power-law EROs have a  $24\mu\text{m}$  detection (14.5 and 16.5). In four out of the five cases of early-type EROs with a  $24\mu\text{m}$  detection, an ACS image is available. In all four cases, a merging galaxy with several close neighbors is apparent. The MIPS point-spread function is  $6''$  so it is possible that the signal in each case might be associated with another galaxy entirely.

We use Le Floch et al. (2005, Fig. 7) to translate our  $24\mu\text{m}$  flux limit (80uJy, 19.1 AB,  $5\sigma$ ) into a lower limit on the total detectable IR luminosity of an ERO in our redshift range. Depending on the model used, at  $z \sim 0.75$ , we are capable of detecting sources more luminous than  $\sim 5 \times 10^{10} L_{\odot}$  i.e., some dusty starbursts, and all LIRGS and ULIRGS. At  $z \sim 1.4$ , we are capable of detecting sources more luminous than  $\sim 5 \times 10^{11} L_{\odot}$  i.e., LIRGS

and ULIRGS. Based on their actual  $24\mu\text{m}$  magnitudes and redshifts, most of our “starburst” sources have intrinsic luminosities between  $10^{11}$  and  $10^{12} L_{\odot}$ , i.e., LIRG class. Both of the “AGN” sources have intrinsic luminosities of  $> 10^{12} L_{\odot}$ , putting them in the ULIRG class.

Although, in this study, we utilized optical/IRAC colors to classify our ERO sample, IRAC-[24] color selection may be a more effective discriminator at higher redshift (Lacy et al. 2004; Ivison et al. 2004; Sajina et al. 2005).

Putting IRAC colors in the context of perhaps more familiar restframe optical colors, Figure 5 shows *restframe*  $U - B$  color versus *observed* [3.6] - [8.0] color for all IRAC-detected galaxies with good [8.0] and good CFHT BRI photometry (see Willmer et al. 2006 for details of the conversion to restframe  $U - B$ ). The symbols are as in Figure 2. The filled circles in Figure 5 denote the 36 EROs which are also detected at  $24\mu\text{m}$  (see also Figure 2). The EROs we classify as early types generally tend to lie on the  $U - B$  defined “red-sequence” and the EROs we classify as dusty starburst tend to lie in the “green valley” and at the top of the “blue cloud” (Weiner et al. 2005).

## 8. CONCLUSIONS

In this paper, we utilized the AEGIS dataset to explore the nature of 87 EROs with confirmed spectroscopic redshifts. IRAC imaging facilitated dividing this sample into three distinct classes using a simple [3.6] - [8.0] color selection technique. We presented SEDs and high-resolution ACS images supporting our (early-type, dusty starburst or power-law) classification.

We showed that the three classes of ERO and their redshift distribution were broadly consistent with what one would expect from a simple color-color diagram (Figure 1). We found 53 early-types, 32 dusty starbursts/LIRGs, and two obvious AGN. Both of these AGN would be classified as ULIRGs.

The selection of this particular sample of EROs was subject to the spectroscopic biases discussed in § 4. We next plan to extend this study to the several thousand IRAC-selected EROs in the AEGIS *without* spectroscopic redshifts.

This work is based in part on observations made with the Spitzer Space Telescope, which is operated by the Jet Propulsion Laboratory, California Institute of Technology under a contract with NASA. Support for this work was provided by NASA through an award issued by JPL/Caltech. ALC is supported by NASA through Hubble Fellowship grant HF-01182.01-A. We thank the referee, Matt Malkan, for constructive comments. GW thanks Mark Lacy, Adam Muzzin, Jason Surace, Ian Smail and Mike Hudson for useful discussions, and UC Berkeley and UC Santa Cruz for their hospitality.

## REFERENCES

- Barmby, P., et al. 2006, *ApJ*, 642, 126  
Coil, A. L., et al. 2004, *ApJ*, 617, 765  
Coleman, G. D., et al., 1980, *ApJS*, 43, 393  
Conselice. 2006, et al., this volume  
Daddi, E., et al., 2004, *ApJ*, 617, 746  
Davis, M., et al., 2006, this volume  
Elston, R., Rieke, G. H., & Rieke, M. J. 1988, *ApJ*, 331, L77  
Faber. 2006, et al., in press  
Fazio, G. G., et al. 2004, *ApJS*, 154, 10  
Franx, M., et al. 2003, *ApJ*, 587, L79  
Huang. 2006, et al., this volume  
Huang, J.-S., et al. 2004, *ApJS*, 154, 44  
Huang, J.-S., et al. 2005, *ApJ*, 634, 137  
Iverson, R. J., et al. 2004, *ApJS*, 154, 124  
Konidaris, N. 2006, et al., this volume  
Lacy, M., et al. 2004, *ApJS*, 154, 166  
Le Flo'c'h, E., et al. 2005, *ApJ*, 632, 169  
Le Flo'c'h. 2006, et al., this volume  
Mannucci, F., 2002, *MNRAS*, 329, L57  
Miyazaki, S., et al. 2002, *PASJ*, 54, 833  
Moustakas, L. A., et al. 2004, *ApJ*, 600, L131  
Papovich, C., et al. 2006, *ApJ*, 640, 92  
Reddy, N. A., Erb, D. K., Steidel, C. C., Shapley, A. E., Adelberger, K. L., & Pettini, M. 2005, *ApJ*, 633, 748  
Rieke, G. H., et al. 2004, *ApJS*, 154, 25  
Rigopoulou. 2006, in press, (astro-ph/0605355)  
Sajina, A., Lacy, M., & Scott, D. 2005, *ApJ*, 621, 256  
Weiner, B. J., et al. 2005, *ApJ*, 620, 595  
Willmer. 2006, et al., in press  
Wilson, G., et al. 2004, *ApJS*, 154, 107  
Wilson, G., Muzzin, A., & Lacy, M. 2005, 'Spitzer Space Telescope: New Views of the Universe' conference (astro-ph/0503638)  
Wilson, G., et al. 2006, 'Spitzer Space Telescope: Infrared Diagnostics of Galaxy Evolution' conference (astro-ph/0604289)

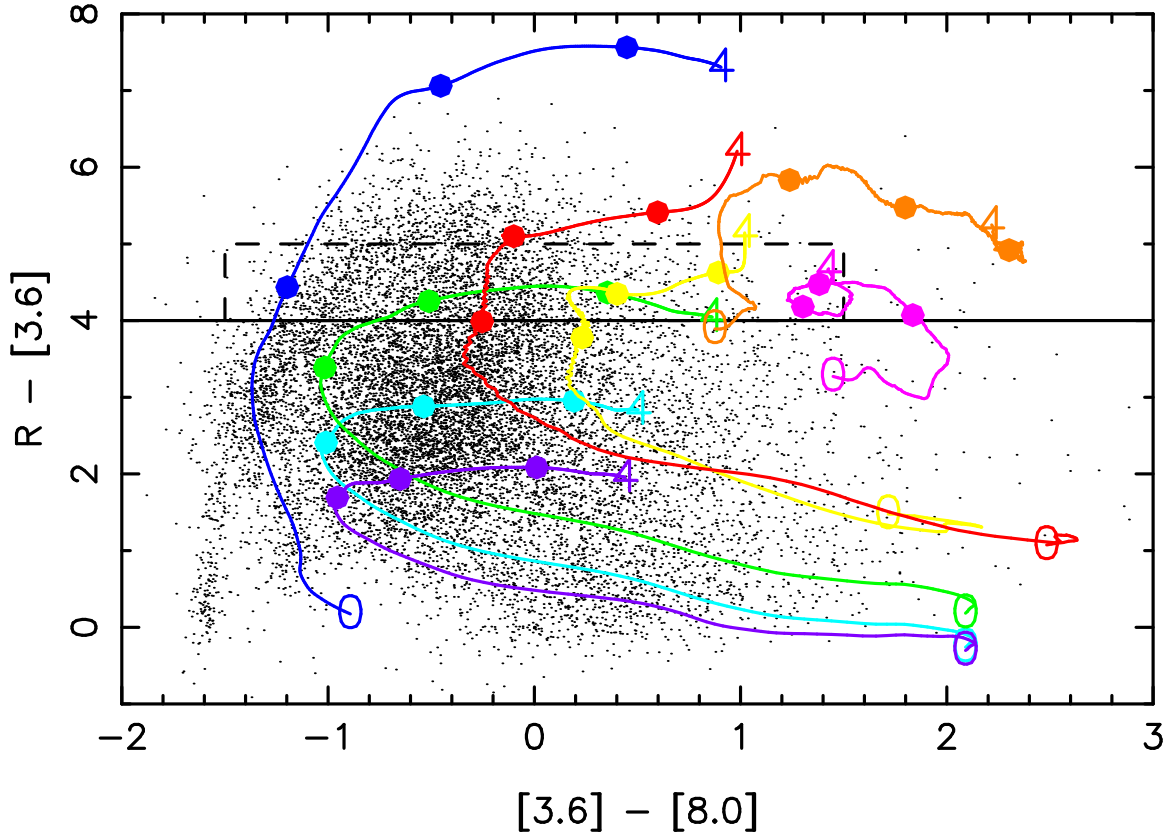


FIG. 1.—  $R - [3.6]$  versus  $[3.6] - [8.0]$  color-color diagram for IRAC-selected galaxies. The solid lines show non-evolving templates in color-color space for CWW early-type (blue), CWW Sbc (green), CWW Scd (cyan), CWW Im (purple), dusty starburst M82 (red), dusty starburst/ULIRG Arp220 (yellow), NGC 1068 (pink) and NGC 5506 (orange). The redshift is indicated for each type. A distinctive swath of galaxies is apparent curving from the left to the top of the Figure. The CWW early-type (blue) track follows this extremely well to  $z \sim 0.7$ , when the template noticeably begins to diverge from the “bluer” data. The plume in the lower left corner is caused by stellar contamination. Galaxies with  $R - [3.6] > 4.0$  (i.e., above the black line) are defined as EROs. One would expect only high redshift ( $z > 0.8$ ) early-type, ( $z > 1.0$ ) dusty starburst galaxies, ( $z > 1.5$ ) CWW Sbc, and AGN (at any redshift) to satisfy this extremely red criterion. The dashed black rectangle indicates the region of color-color space populated by the 87 EROs with confirmed spectroscopic redshifts (see also right panel of Figure 2 and § 5).

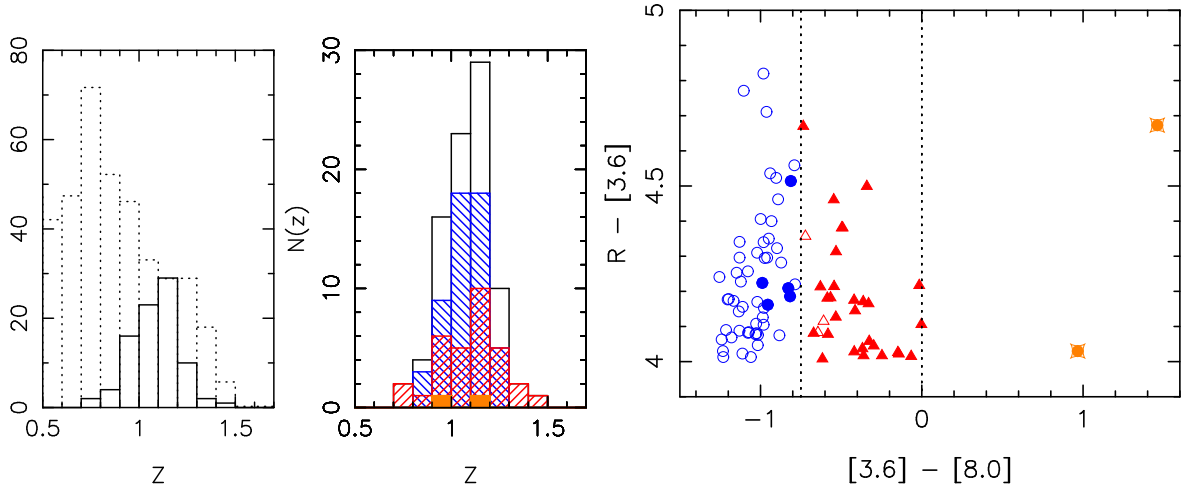


FIG. 2.— The solid black histogram in the far left panel shows the ERO redshift distribution  $N(z)$  (which peaks for this sample of 87 EROs at  $z = 1.15$ ). The dotted black line illustrates the underlying DEEP2 selection function in the EGS field *before* the ERO criterion is applied. The dotted black line shows the redshift distribution  $N(z)$  of all 6023 galaxies with good quality redshift determinations, scaled down by a factor of 15 for comparison with the ERO  $N(z)$ . The right panel (dashed black rectangle in Figure 1) shows our IRAC  $[3.6] - [8.0]$  color division into early type (blue circles), dusty starburst (red triangles) and power-law (orange boxes) EROs. Filled symbols indicate the 36 EROs with a  $24\mu\text{m}$  detection (19.1 AB,  $5\sigma$ , § 7). Also shown in the middle panel (and discussed in § 5), is the redshift distribution of the full sample (black) and the three sub-classes (using the same blue, red and orange color scheme).

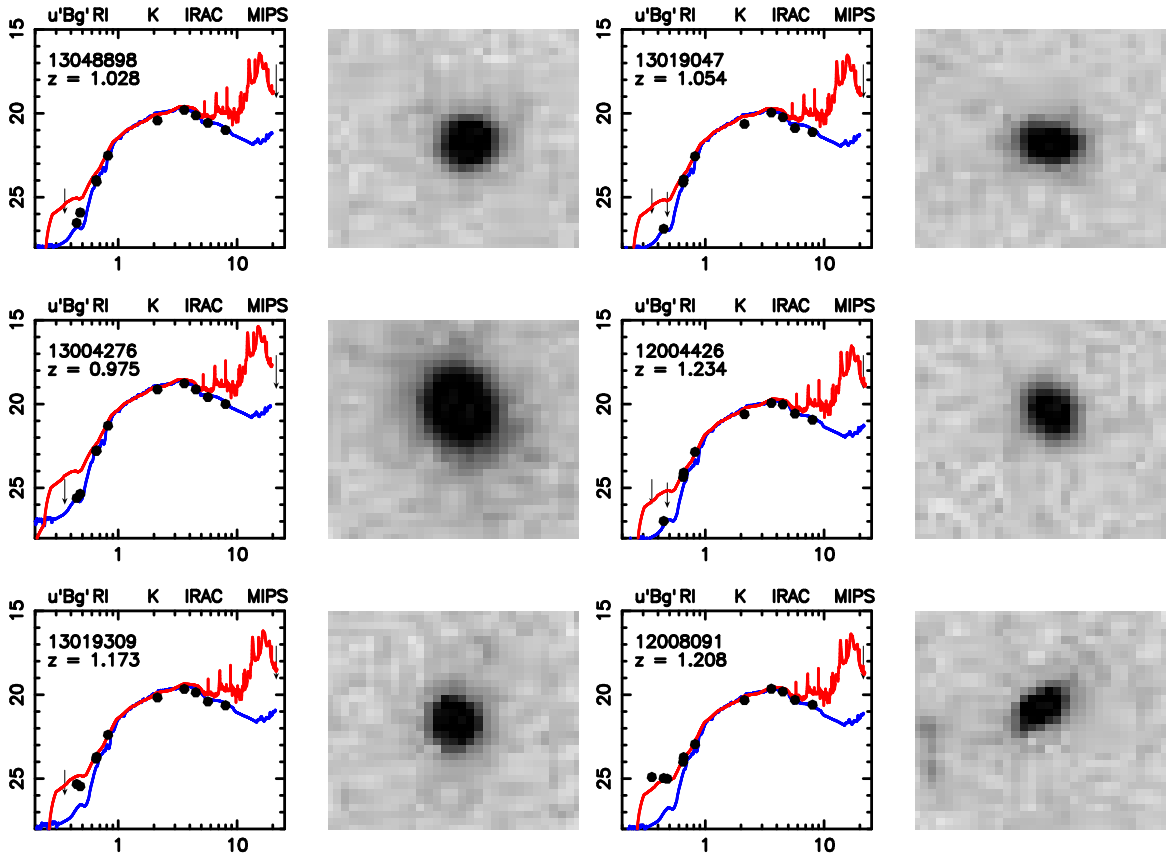


FIG. 3.— Examples of observed SEDs (left) and  $3'' \times 3''$   $I$ -band ACS images (right) for six IRAC color-selected early-type EROs. A maximum of 12 passbands ( $u'$ ,  $B$ ,  $g'$ , Subaru  $R$ , CFHT  $R$ ,  $I$ ,  $K$  [3.6], [4.5] [5.8], [8.0] and [24.0]) are shown. The tip of the downward pointing arrow indicates upper limits in the case of non-detections. Each panel shows the DEEP2 ID number, and the spectroscopic redshift. Also shown are a CWW E (blue) and M82 (red) template (§ 3) as they would appear at the redshift of each ERO. See § 6 discussion.

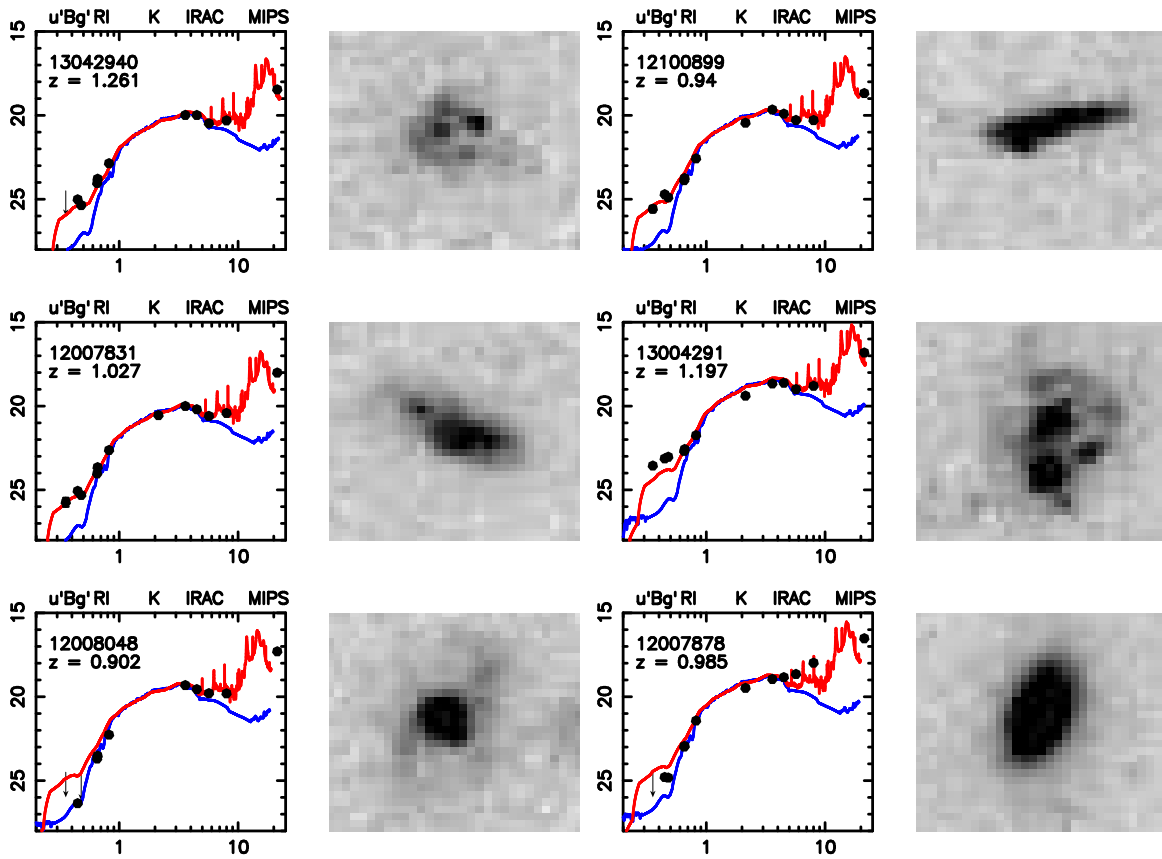


FIG. 4.— As for Figure 3, but for five IRAC color-selected dusty starburst EROs and one power-law ERO (12007878). The M82 dusty starburst template approximates the 13042940, 12100899, and 12007831 SEDs very well, and that of 13004291 reasonably well. In most cases the ACS images show clear evidence of interactions and mergers. 12008048 is a face-on dusty spiral galaxy.



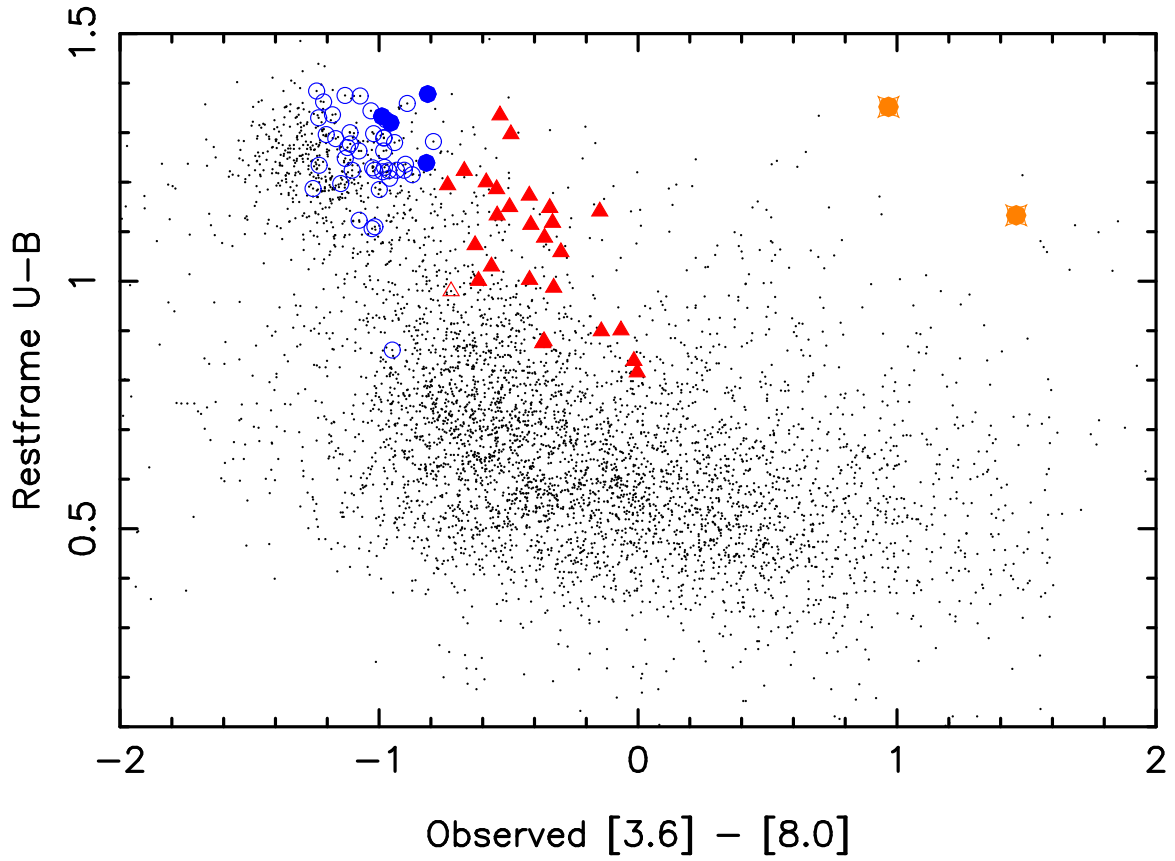


FIG. 5.— Restframe  $U - B$  color versus observed  $[3.6] - [8.0]$  color for all IRAC-detected galaxies with good  $[8.0]$  and good CFHT BRI photometry. Note:  $(U - B)_{\text{Vega}} = (U - B)_{\text{AB}} - 0.85$ . Blue circles indicate bulge-dominated early-type EROs. Red triangles indicate dusty starburst EROs. Orange boxes indicate the two AGN. Filled symbols indicate a  $24\mu\text{m}$  detection. It is possible that the  $24\mu\text{m}$  detections associated with each of the early-type EROs may be spurious, and actually associated with a close neighbor galaxy (see § 7). The early-type EROs generally tend to lie on the  $U - B$  defined red-sequence and the dusty starburst EROs lie in the “green valley” and at the top of the “blue cloud”.